Biomedicine & Pharmacotherapy 109 (2019) 1728–1739

Contents lists available at ScienceDirect

Biomedicine & Pharmacotherapy

journal homepage: www.elsevier.com/locate/biopha

Investigation of the antitumor activity and toxicity of long-circulating and fusogenic liposomes co-encapsulating paclitaxel and doxorubicin in a murine breast cancer animal model

Marina Santiago Franco[a], Marjorie Coimbra Roque[a], André Luís Branco de Barros[b], Juliana de Oliveira Silva[a], Geovanni Dantas Cassali[c], Mônica Cristina Oliveira[a,*]

[a] Department of Pharmaceutical Products, Faculty of Pharmacy, Universidade Federal de Minas Gerais, Av. Antônio Carlos, 6627, 31270-901, Belo Horizonte, Minas Gerais, Brazil
[b] Department of Toxicological and Clinical Analyses, Faculty of Pharmacy, Universidade Federal de Minas Gerais, Av. Antônio Carlos, 6627, 31270-901, Belo Horizonte, Minas Gerais, Brazil
[c] Department of General Pathology, Institute of Biological Sciences, Universidade Federal de Minas Gerais, Av. Antônio Carlos, 6627, 31270-901, Belo Horizonte, Minas Gerais, Brazil

ARTICLE INFO

Keywords:
Co-delivery
Cytotoxicity
Nuclear morphometric analysis
Migration assay
Cardiotoxicity
Antitumor efficacy

ABSTRACT

To associate paclitaxel (PTX) with doxorubicin (DXR) is one of the main chemotherapy strategies for breast cancer (BC) management. Despite the high response rates for this combination, it presents a cardiotoxic synergism, attributed to pharmacokinetic interactions between PTX and both DXR and its metabolite, doxorubicinol. One of the main strategies to minimize the cardiotoxicity of the combination is to extend the interval of time between DXR and PTX administration. However, it has been previously suggested that their co-administration leads to better efficacy compared to their sequential administration. In the present study, we investigated different molar ratio combinations of PTX:DXR (10:1; 1:1, and 1:10) against the 4T1 murine breast cancer cell line and concluded that there is no benefit of enhancing PTX concentration above that of DXR on the combination. Therefore, we obtained a long-circulating and fusogenic liposomal formulation co-encapsulating PTX and DXR (LCFL-PTX/DXR) at a molar ratio of 1:10, respectively, which maintained the *in vitro* biological activity of the combination. This formulation was investigated for its antitumor activity and toxicity in Balb/c mice bearing 4T1 breast tumor, and compared to treatments with free PTX, free DXR, and the mixture of free PTX:DXR at 1:10 molar ratio. The higher tumor inhibition ratios were observed for the treatments with free and co-encapsulated PTX:DXR in liposomes (66.87 and 66.52%, respectively, $P > 0.05$) as compared to the control. The great advantage of the treatment with LCFL-PTX/DXR was its improved cardiac toxicity profile. While degeneration was observed in the hearts of all animals treated with the free PTX:DXR combination, no signs of cardiac toxicity were observed for animals treated with the LCFL-PTX/DXR. Thus, LCFL-PTX/DXR enables the co-administration of PTX and DXR, and might be considered valuable for breast cancer management.

1. Introduction

Breast cancer (BC) is the most frequent cancer among women. In less developed regions, BC is the leading cause of cancer death in women while in more developed regions it is second to lung cancer [1]. The mortality rates are declining due to the treatment options currently available for BC management [2]. Among these treatments, the most effective chemotherapy regimens are those based on anthracyclines. The incorporation of taxanes in these regimens further improves patient outcomes in the neo/adjuvant setting [3,4]. Despite their efficacy, the potential long-term sequelae of the cardiotoxicity of anthracycline-based therapy are of particular concern. Survivors of BC might suffer the consequences of these regimens more than 10 years after their administration, becoming a complex group of patients as BC turns from a life-threatening illness to a chronic condition [5,6]. This highlights the need to search for new therapeutic strategies. Cancer nanomedicine aims to overcome the intrinsic limits of conventional cancer therapies in order to provide more effective and safer treatments [7–10]. Some nanosystems, such as Doxil®, a liposomal formulation of doxorubicin (DXR), and Abraxane®, nanoparticle albumin-bound paclitaxel (PTX), are already widely and successfully used for clinical treatment of BC [11]. A

* Corresponding author.
E-mail address: monicacristina@ufmg.br (M.C. Oliveira).

https://doi.org/10.1016/j.biopha.2018.11.011
Received 19 July 2018; Received in revised form 1 November 2018; Accepted 2 November 2018

new strategy in nanomedicine that started attracting significant attention in the first decade of this century is the development of nanosystems designed to co-encapsulate drugs in synergistic ratios, as recently reviewed by Franco and Oliveira [12,13]. This strategy was derived from the fact that synergism or antagonism against the same tumor cells *in vitro* can be observed for the same anticancer drug combinations depending only on the ratios in which these agents are combined. This finding highlighted the idea that maybe the full potential of the chemotherapy regimens used in the clinics is being wasted, as the ratio of the drugs reaching the tumor was never a concern. Upon the administration of free drugs, the ratio of the agents reaching the tumor is completely arbitrary, due to their dissimilar pharmacokinetics [14]. Therefore, the need to control drug ratios reaching the tumor site presents a great challenge, and the ratiometric drug delivery using nanocarriers turns out to be a promising strategy [12,13]. Different liposomal formulations designed upon this strategy have shown the ability to maintain drug ratios in the plasma after injection as well as to deliver the desired drug ratio directly to the tumor tissue, ensuring a faithful translation of the *in vitro* effects to *in vivo* [15–20]. This strategy was validated in 2017 upon FDA approval of Vyxeos®, a liposomal formulation co-encapsulating a fixed ratio of cytarabine:daunorubicin, for acute myeloid leukemia treatment [21,22].

In the present work, we evaluated the effects of free PTX, free DXR, and their combinations (PTX:DXR) at molar ratios of 10:1, 1:1, and 1:10 on cell viability, nuclear morphology, and migration of the 4T1 murine breast cancer cell line. The results allowed us to suggest that there is no benefit of enhancing PTX concentration above that of DXR in the combinations. Cell viability evaluation after exposure to long-circulating and fusogenic liposomal formulation co-encapsulating PTX and DXR (LCFL-PTX/DXR) at the molar ratio of 1:10, respectively, revealed that the biological activity of the combination was maintained after its encapsulation. The physico-chemical properties and *in vitro* release profile of this formulation were previously investigated by our research group. Results revealed that LCFL-PTX/DXR presents adequate parameters for intravenous administration and the simultaneous release of both drugs maintaining the desired 1:10 molar ratio of PTX:DXR for up to 36 h [23]. Therefore, we proceeded herein with investigating the antitumor activity and toxicity of LCFL-PTX/DXR in Balb/c mice bearing the 4T1 breast tumor and comparing it to treatments with free PTX in two different doses, free DXR and the mixture of free PTX:DXR at a 1:10 molar ratio.

2. Materials and methods

2.1. Materials

The lipids 1,2-dioleoyl-sn-glycero-3-phosphoethanolamine (DOPE) and 1,2-distearoyl-sn-glycero-3-phosphoethanolamine-N-[amino(polyethyleneglycol)-2000(DSPE-PEG_{2000}) were supplied by Lipoid GmbH (Ludwigshafen, Germany). Cholesterol hemisuccinate (CHEMS), doxorubicin (DXR), 4-(2-hydroxyethyl)-1-piperazine ethanesulfonic acid (HEPES) sodium salt, sodium chloride, sodium hydroxide and Cremophor EL, RPMI culture media, fetal bovine serum, penicillin/streptomycin and 3-(4,5 dimethylthiazolyl-2)-2,5-diphenyltetrazolium bromide (MTT) were obtained from Sigma-Aldrich Co. (St Louis, MO, USA). Paclitaxel (PTX) was supplied by Quiral Quimica do Brasil S.A (Juiz de Fora, Brazil). The 4T1 murine breast carcinoma cell line was purchased from American Type Culture Collection (Manassas, VA, USA). All other chemicals used in this study were of analytical grade.

2.2. Liposome preparation

LCFL-PTX/DXR was prepared by the lipid film hydration technique, as described elsewhere [23]. Briefly, DOPE, CHEMS, and DSPE-PEG2000 (at 5.7:3.8:0.5 molar ratio, respectively) were dissolved in chloroform at 10 mmol L^{-1} total lipid concentration, mixed with PTX (0.25 mg/mL) in a round bottom flask and submitted to evaporation under reduced pressure in a 50 °C water bath until a thin lipid film was obtained. The round bottom flask containing the lipid film was then maintained for 1 h under a chloroform atmosphere for better dispersion of PTX in the lipids, according to the technique known as annealing [24]. A solution of ammonium sulphate (300 mM, pH 7.4) preheated to 50 °C was then added to the film and the mixture was kept in an ultrasonic bath at 50 °C for 10 min for its hydration. Non-entrapped PTX was eliminated by centrifugation at 3000 rpm, 25 °C, for 10 min (Heraeus Multifuge X1R centrifuge, Thermo Fischer Scientific, Massachusetts, USA). To remove non-entrapped ammonium sulfate, liposomes were maintained on dialysis overnight against HEPES buffered saline (HBS), pH 7.4. PTX concentration in these liposomes was determined by high performance liquid chromatography (HPLC) analysis. After determination of the PTX concentration, DXR was remotely loaded into liposomes driven by the transmembrane ammonium sulphate gradient in order to obtain the PTX:DXR molar ratio of 1:10. For that, the liposomes containing PTX were incubated with DXR for 2 h at 25 °C. To remove non-entrapped DXR, liposomes were submitted to another dialysis against HBS at pH 7.4, overnight.

2.3. Liposome characterization

2.3.1. Determination of the diameter, polydispersity index, and zeta potential

The diameter of the vesicles and the polydispersity index (PI) were determined by dynamic light scattering (DLS). The measurements were performed at a temperature of 25 °C, using a 90° laser incidence angle. The zeta potential (ζ) of the vesicles was determined by DLS associated with electrophoretic mobility. To perform both measurements, the liposomes were diluted in HBS, pH 7.4, and evaluated on the Zetasizer Nano ZS90 equipment (Malvern, England).

2.3.2. Determination of the content of PTX and DXR

The PTX concentration was determined by high-performance liquid chromatography (HPLC, Waters Instruments, Milford, USA). The mobile phase was composed of 55% acetonitrile in water. The elution time was 8 min, and the Hibar 250-4 LiChrospher 100RP-18, 25 cm x 4 mm, 5 µm column (Merck, Darmstadt, Germany) was used. The column was kept at room temperature, the flow rate was set at 1.2 mL/min, and the detection wavelength was 227 nm. UV-VIS spectrophotometry (Thermo evolution 201 UV visible spectrophotometer) was used as the DXR assay method. The analyses were performed to evaluate the absorbance at wavelength equal to 480 nm. Initially, the lipid vesicles were opened with isopropyl alcohol at a volume ratio equal to 1:2, respectively, and then the preparations were diluted in HBS buffer, pH 7.4. The PTX and DXR encapsulation percentage (EP) was calculated according to the following equation:

$$EP = \frac{[amount\ of\ drug\ in\ purified\ liposomes]}{[amount\ of\ drug\ in\ the\ non\ purified\ liposomes]} \times 100$$

2.4. Cell culture

The 4T1 murine breast carcinoma cell line was cultivated in RPMI supplemented with 10% FBS, in the presence of penicillin (100 U/mL) and streptomicin (100 µg/mL), and maintained at 37 °C and 5% CO_2 in a humidified atmosphere. Prior to the experiments, the cell line was screened for mycoplasma by polymerase chain reaction (PCR), with negative results.

2.5. MTT assay

The MTT assay was chosen as the means of evaluating 4T1 cell viability after exposure to the determined concentrations of different treatments. For that, cells were plated in a density of 5×10^3 cells per well in 96-well plates, and kept in the incubator for around 24 h prior to exposition to the treatments. Then, cells were exposed to 5 different concentrations (0.625; 1.25; 2.5; 5, and 10.0 mM) of PTX, DXR, mixture of PTX:DXR at different molar ratios (10:1; 1:1, and 1:10), and LCFL-

PTX/DXR co-encapsulating PTX:DXR at a 1:10 molar ratio for 48 h. After incubation time, treatments were removed and 100 μL of MTT (0.5 mg/mL) were incubated for 1 h at 37 °C. After incubation time, media containing MTT was removed from the wells and 100 μL of DMSO was added to solubilize the formazan crystals. The absorbance of the wells was determined using a bench spectrophotometer model Benchmark Plus (Bio-Rad, California, USA) at 570 nm. All experiments were performed in duplicate of wells per concentration and triplicate of plates. The test data were converted to mean fraction of cell survival relative to untreated cells (control group). The data were analyzed by nonlinear regression to obtain the IC_{50} values.

2.6. Nuclear morphometric analyses

To evaluate nuclear morphological alterations after treatments, 4T1 murine breast carcinoma cells were plated at a density of 2.0×10^5 cells/well in 6-well plates and incubated at 37 °C for 24 h. After incubation time, cells were treated for 48 h with 2 mL of different treatments at concentration of 700 nM (PTX, DXR, and the mixtures of free PTX:DXR at 10:1; 1:1, or 1:10 molar ratio). After incubation, the cells were fixed with formaldehyde 4% for 10 min. Fixed cells were stained with Hoescht 33342 (0.2μg/mL) solution for 10 min at room temperature in the dark. Nuclei fluorescence images were captured using a microscope AxioVert 25 with a fluorescence module Fluo HBO 50 connected to the Axio Cam MRC camera (Zeiss, Oberkochen, Germany). A total of 100 nuclei per treatment were analyzed using the Software Image J 1.50i (National Institutes of Health, Bethesda, USA) and the plugin "NII_Plugin" available at http://www.ufrgs.br/labsinal/NMA/.

2.7. Migration assay

To study the bi-dimensional migration of the different cell lines, they were plated at a density of 2.0×10^5 cells/well in 12-well plates and incubated at 37 °C for 24 h. Then, a straight wound was made in individual wells with a 10 mL pipette tip. This point was considered the "0 h," and the "zero wound" was photographed using a microscope AxioVert 25 with a connected Axio Cam MRC camera (Zeiss, Oberkochen, Germany). After obtaining the wounds, control wells received fresh media and the other wells received 1 mL of media containing the different treatments at a concentration of 700 nM (PTX, DXR, and the mixtures of free PTX:DXR at 10:1; 1:1, or 1:10 molar ratio). The plates were incubated at 37 °C for 24 h. In these experiments, from the plating moment until the end of the assays, the cells were kept in starvation, meaning the different media contained only 1% FBS. After incubation, the cells were fixed with formaldehyde 4% for 10 min. Images along the wounds of control and treated groups were obtained in phase contrast. Wound areas were obtained using the MRI Wound Healing Tool plugin for the free version of Image J 1.45 software (National Institutes of Health, Bethesda, USA). The wound healing percentage was calculated according to the following equation:

$$\%\,wound\quad healing = 100 - \frac{(area\quad of\quad treated\quad wound\quad \times\quad 100)}{area\quad of\quad the\quad "zero\quad wound"}$$

2.8. Animals

Balb/c female mice, 6–7 weeks old, weighing 18.0 ± 2.0 g, were obtained from the Central Animal House of the Universidade Federal de Minas Gerais, Brazil. The animals were kept in plastic cages with free access to food and water and under standardized light/dark cycle conditions. All protocols were approved by the Ethics Committee for Animal Experiments from the Universidade Federal de Minas Gerais, and are in compliance with the guidelines for the care and use of laboratory animals recommended by the Institute of Laboratory Animal Resources (Protocol number 6/2016).

2.9. Antitumor activity evaluation

Mice were inoculated subcutaneously in the right flank with 2.5×10^6 4T1 murine breast carcinoma cells and one week later were randomly divided into six experimental groups. Different groups received four doses of the different treatments intravenously through the tail vein every three days. The treatments consisted of NaCl 0.9% (w/v) solution, free PTX at two different doses (0.85 mg/kg or 8.54 mg/kg), free DXR (5.45 mg/kg), free PTX:DXR at a 1:10 molar ratio (PTX 0.85 mg/kg + DXR 5.45 mg/kg), and LCFL-PTX/DXR (PTX 0.85 mg/kg + DXR 5.45 mg/kg). The number of animals was equal to seven in groups treated with NaCl 0.9% (w/v) or LCFL-PTX/DXR, and six in the other groups. The first day on which the formulations were administered was considered day 0 (D0) of the study. As such, the formulations were administered on D0, D3, D6, and D9, and mice were euthanized three days after the last treatment, on D12. The length and width of the tumor were measured with a fine caliper (Mitutoyo, MIP/E-103) on D0, D3, D6, D9, and D12. The tumor volume was expressed as $0.52 \times (length \times width^2)$ [25]. Antitumor activity was evaluated over the 12-day period and the tumor growth inhibition ratio was calculated.

The inhibition ratio (IR) was calculated on D12, as follows:

$$IR\% = 1 - \frac{Mean\quad RTV\quad of\quad drug\quad treated\quad group}{Mean\quad RTV\quad of\quad control\quad group} \times 100$$

Where, $RTV\quad (relative\quad tumor\quad volume) = \frac{Tumor\quad volume\quad on\quad D12}{Tumor\quad volume\quad on\quad D0}$

2.10. Tumor histology and metastasis evaluation

The 4T1 breast tumor-bearing mice were anesthetized with a mixture of xylazine (15 mg/kg) and ketamine (80 mg/kg) on D12, and euthanized; and then the tumor, heart, lungs, kidneys, spleen, and liver were removed for histopathological evaluation. The tissues were fixed in 10% (v/v) buffered formalin, embedded in paraffin blocks, sectioned into a 5 μm thickness, placed onto glass slides, and stained with hematoxylin-eosin. The sections were examined by an experienced pathologist, who was blinded to the treatment type during the analysis. Metastatic lung nodules were quantified in one lung cross-section at the midsection through the block for each mouse assessed. The images were captured with a microcamera (Spot Insight Color; SPOT Imaging Solutions, Sterling Heights, MI, USA) attached to a microscope (Olympus BX-40; Olympus, Tokyo, Japan).

2.11. Determination of the effect of the different treatments on serum vascular endothelial growth factor levels

Blood was collected from the braquial plexus of Balb/c female mice bearing 4T1 breast tumor on D12. The plasma was collected by centrifuging blood at 2500 × *g* for 10 min, and the plasma vascular endothelial growth factor (VEGF) levels were measured using a mouse VEGF ELISA kit (DuoSET ELISA mouse VEGF; R&D Systems, Minneapolis, MN, USA), according to the manufacturer's protocols.

2.12. Toxicity evaluation

Toxicity of the different treatments was assessed by evaluating mice body weight changes, hematological parameters, and the histopathology of different organs. Mice body weight was monitored on D0, D3, D6, D9, and D12. Weight variations were expressed as the percentage of the initial body weight. For hematological analyses, the whole blood was collected from the brachial plexus in tubes containing EDTA on D12. The analyses of the hematological parameters, including white and red blood cell count, hemoglobin concentration, hematocrit, and platelet count, were performed on Hemovet 2300 equipment (Brasmed Veterinária, São Paulo, SP, Brazil). For histopathological analyses of the heart, lungs, kidneys, spleen, and liver to investigate the

toxicity, sections of these organs were prepared and stained, and images were captured as described in Section 2.10.

2.13. Statistical analyses

The results were expressed as mean ± SD of three independent experiments. Statistical analyses were performed by one-way ANOVA followed by Tukey's post-test. Prior to ANOVA analyses, data concerning NMA and scratch assay were transformed as y = square root (value) and data concerning tumor volume and number of pulmonary metastasis were transformed as y = log (value) to fit the normality and homocedasticity requirements, which were evaluated by Kolmogorov-Smirnov and Levene tests, respectively. Differences were considered statistically significant when P values were < 0.05. GraphPad Prism 5.04 Software (GraphPad, USA) was used to calculate all data.

3. Results

3.1. Physicochemical characterization of the different liposomal formulations

LCFL-PTX/DXR presented a mean diameter of 262.0 ± 22.9 nm. The mean PI value was 0.26 ± 0.02, indicating that the vesicle population in the formulation was monodisperse. Zeta potential mean value was −6.2 ± 2.5 mV, near the neutrality, as expected for a formulation containing PEG on its bilayer [26]. Besides, the use of a gradient to encapsulate DXR allowed for the obtainment of a formulation with a PTX:DXR molar ratio close to the desired, 1:10, with mean PTX concentration of 0.17 ± 0.04 mg/mL and mean DXR concentration of 0.94 ± 0.22 mg/mL. These results are in accordance with those previously reported by our research group [23].

3.2. MTT assay

PTX presented a cytotoxicity plateau for the dose range evaluated herein, as observed in Fig. 1, so that it was not possible to calculate the IC50 value of this treatment against the 4T1 cell line. This cytotoxicity plateau has been previously reported for different cell lines exposed to the PTX treatment or other components that disrupt microtubule function [27]. An IC_{50} value of 2.27 ± 0.13 μM was calculated for the treatment with PTX:DXR at a 10:1 molar ratio, statistically superior to that observed for free DXR treatment (1.49 ± 0.02 μM, $P < 0.05$). Treatments with the free mixture of PTX:DXR at molar ratios of 1:1 and 1:10 had IC_{50} values of 0.74 ± 0.05 and 0.76 ± 0.05 μM, respectively, while that with LCFL-PTX/DXR had an IC_{50} value of 0.83 ± 0.04 μM. The IC_{50} values of all these treatments were statistically lower compared to that of free DXR treatment ($P < 0.05$) and did not differ statistically between them ($P > 0.05$).

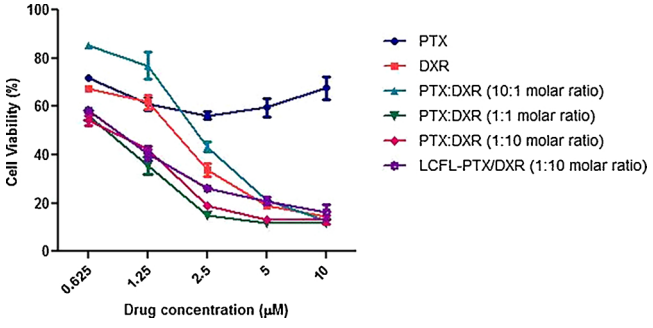

Fig. 1. Concentration-response curve of 4T1 cells after exposition to different treatments for 48 h. Data shown represent the mean ± SD of three independent experiments.

3.3. Nuclear morphometric analyses

Knowing that several cellular processes can be inferred by the analysis of nuclear morphometric features, Filippi-Chiela and coworkers (2012) developed the "Nuclear Morphometric Analysis (NMA) tool," which divides nuclei into six groups according to their morphological appearances. Each of these morphological characteristics has a putative biological meaning: normal (N), irregular (I, mitotic catastrophe or other nuclear damaging event), small regular (SR, apoptosis in an early or intermediary stage), small (S, mitosis), small irregular (SI, mitosis with damage or nuclear fragments), large regular (LR, senescence), and large irregular (LI, mitotic catastrophe or other nuclear damaging event) [28]. In the present study, the morphometric analysis of nuclei size and irregularity of the 4T1 cell line showed that the exposure to the PTX treatment resulted in similar amounts of LR and LI + I nuclei (39 and 42%, respectively). Nuclear irregularities are characteristic of mitotic catastrophe or other nuclear damaging event, and are expected to be present in higher extension after treatments containing higher concentrations of microtubule-hyperpolymerizing agents, such as PTX, as these drugs particularly result in further damage leading to mitotic catastrophe [29–31]. All other treatments resulted predominantly in an increase in the percentage of LR nuclei (ranging from 62 to 70%), followed by LI + I nuclei (ranging from 17 to 22%), as shown in Fig. 2. Nuclear enlargement as herein observed is a characteristic of cancer cell senescence, a state of cellular arrest that frequently occurs in response to the therapy. It is often called therapy-induced senescence (TIS) or accelerated cellular senescence to differentiate from the aging process of normal cells known as replicative senescence [32,33]. Fig. 3 presents fluorescence photomicrographs of Hoescht 33342 stained 4T1 nuclei, where nuclear enlargement for cells exposed to the different treatments is evident when compared to untreated cells.

3.4. Migration assay

The wound healing assay allows the observation of two-dimensional (2D) cell migration in confluent monolayer cell cultures [34]. To guarantee that the wound closures observed were due exclusively to the cell migration and not cell proliferation, the experiments were performed in lower FBS concentration (1%). This procedure is known as cell starvation, and aims to suppress proliferation [35]. Additionally, wound closures were evaluated 24 h after exposure to the different treatments. Longer study periods do not allow distinguishing cell proliferation and changes in cell survival from the cell motility [36]. All treatments containing PTX significantly reduced the percentage of cell migration compared to the control group ($P < 0.05$), which was expected since microtubule-affecting drugs are known to present significant antimigratory properties of tumor cells [37]. When cells were treated with PTX, the percentage of migration in relation to the control (PM) was 55.1 ± 10.9. No difference in migration ($P > 0.05$) was observed between PTX treatment alone and the combinations of PTX:DXR on molar ratios of 10:1 (PM = 60.6 ± 9.9); 1:1 (PM = 40.7 ± 9.3); and 1:10 (PM =

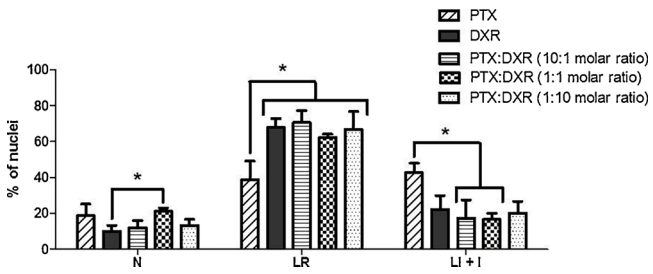

Fig. 2. Nuclear morphometric distribution of 4T1 breast cancer cell nuclei exposed to 700 nM of different treatments for 48 h. Data shown represent the mean ± SD of three independent experiments. * = groups differ statistically, ANOVA, $p < 0.05$.

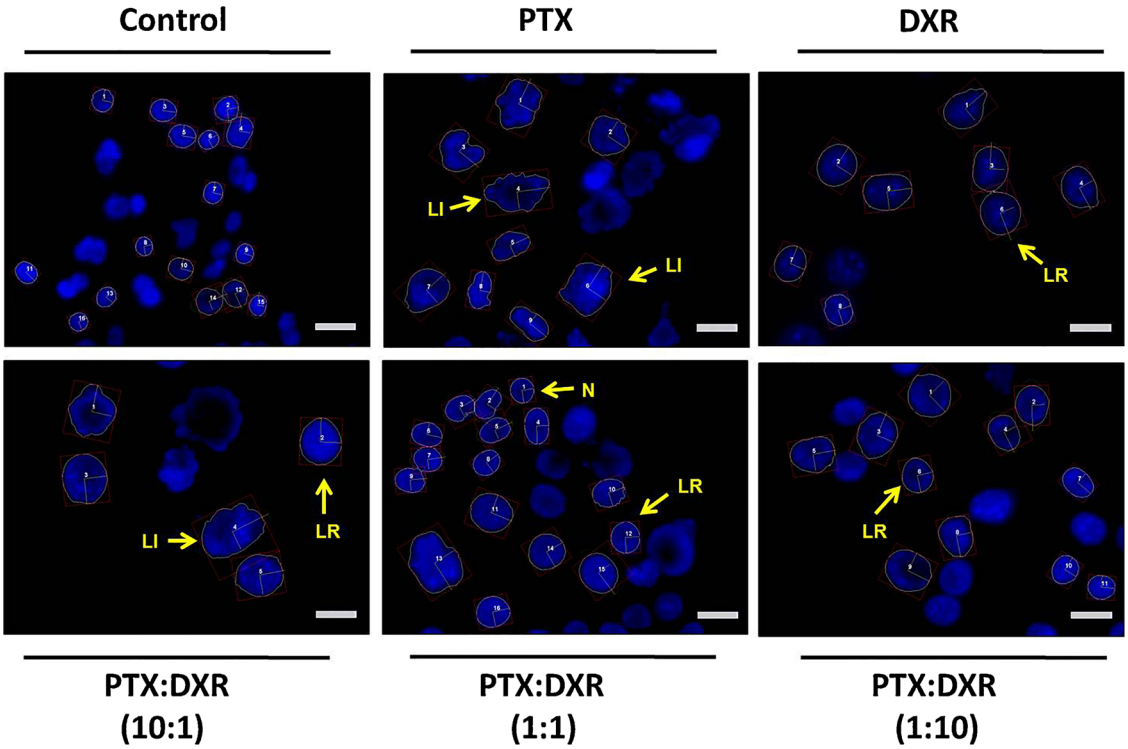

Fig. 3. Fluorescence photomicrographs of 4T1 breast cancer cell nuclei stained with Hoescht 33342 after different treatments at concentration of 700 nM for 48 h. Some of the different nuclei morphometric phenotypes observed are indicated. N, normal; LI, large irregular; LR, large regular. Images are representative of three independent experiments. Amplification 40×, scale bar = 20 μm.

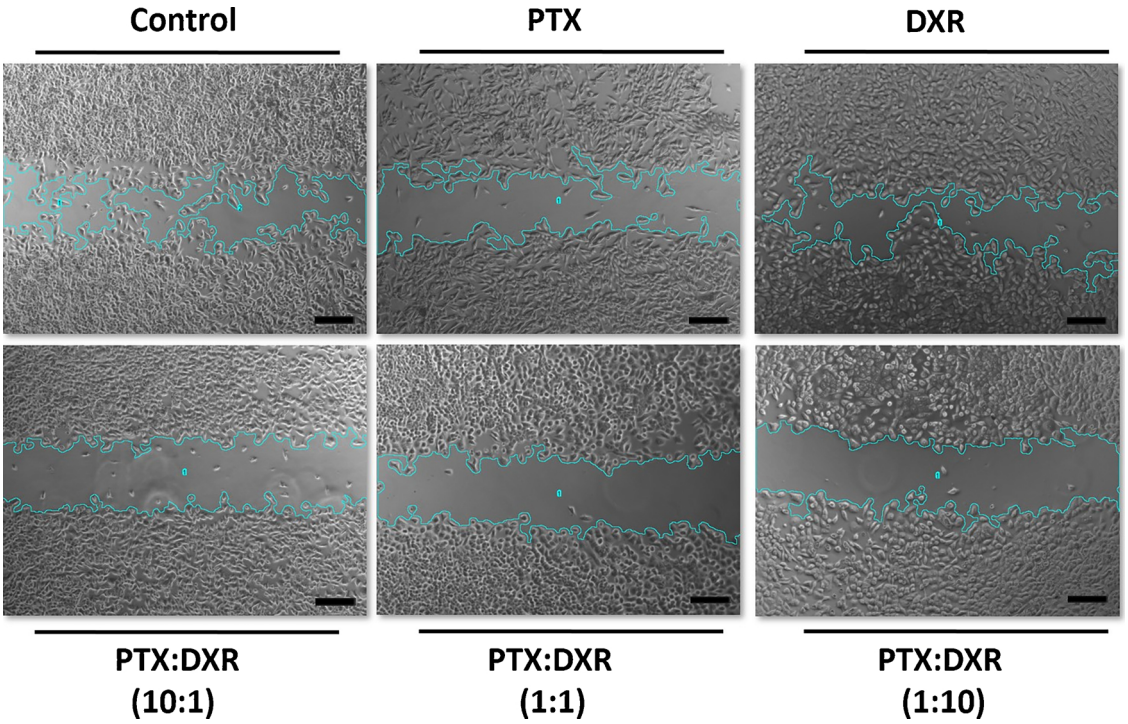

Fig. 4. Phase-contrast photomicrographs of the wounds of 4T1 breast cancer cells on control group or exposed to 700 nM of the different treatments for 24 h. Images are representative of three independent experiments. Amplification 5×, scale bar = 200 μm.

51.9 ± 11.9). Treatment with DXR did not suppress 4T1 cell migration (PM= 88.8 ± 8.3), which did not differ statistically from the migration observed for the control group ($P > 0.05$). Representative phase-contrast photomicrographs of the scratches after 24 h of exposure to the treatments are presented in Fig. 4.

3.5. Antitumor activity evaluation

All treatments suppressed the tumor growth at D12 as compared to the control group ($P < 0.05$) (Fig. 5). The increase in the dose of PTX by 10-fold (8.54 mg/kg) allowed for the tumor suppression to appear

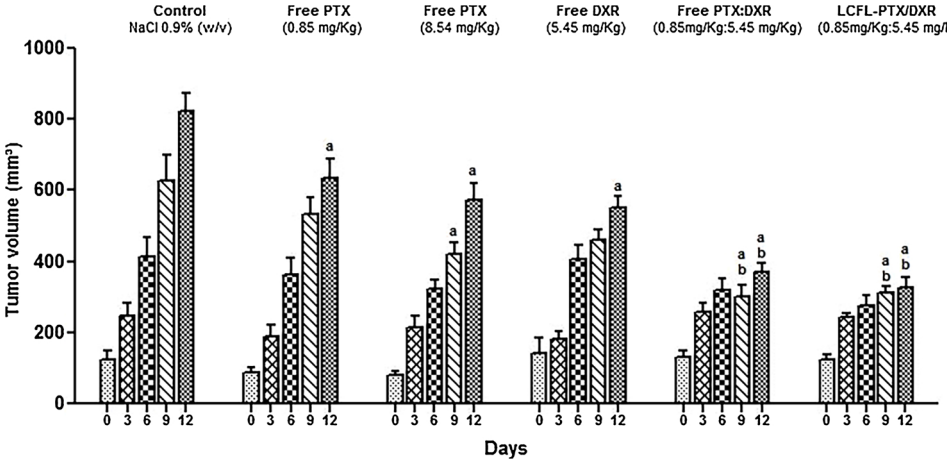

Fig. 5. Determination of the tumor volume after intravenous administration of NaCl 0.9% (w/v), free PTX (0.85 mg/kg or 8.54 mg/kg), free DXR (5.45 mg/kg), free mixture of PTX:DXR and LCFL-PTX/DXR at 1:10 molar ratio (PTX 0.85 mg/kg + DXR 5.45 mg/kg) to Balb/c female mice transplanted subcutaneously with 4T1 breast cancer cells. Administrations of different treatments occurred on days 0, 3, 6 and 9. Data shown represent the mean ± SEM. The number of animals was equal to seven in groups treated with NaCl 0.9% (w/v) or LCFL-PTX/DXR, and six in the other groups. [a] = differs statistically from control group; [b] = differs statistically from free DXR treatment. ANOVA, $p < 0.05$.

earlier (D9) in the study, but did not increase its efficacy at the end of the experiment compared to the treatment with low dose of PTX (0.85 mg/kg, $P > 0.05$). The IR calculated for free PTX treatment administered at 0.85 mg/kg and 8.54 mg/kg were 17.5 and 18.4, respectively (Table 1). For free DXR treatment (5.45 mg/kg), the IR was equal to 37.6, indicating a better antitumor activity compared to the treatments with free PTX alone in different doses. The combination of the treatments with PTX and DXR further improved the antitumor activity, once the animals treated with the mixture of free PTX:DXR and LCFL-PTX/DXR (PTX 0.85 mg/kg + DXR 5.45 mg/kg) presented significantly smaller tumors on D9 and D12 as compared to those treated with free DXR alone ($P < 0.05$). During the whole experiment, no significant difference was observed in the tumor volume of animals receiving either free mixture of PTX:DXR or LCFL-PTX/DXR ($P < 0.05$). The IR calculated for these treatments was equal to 66.9 and 66.5, respectively. We suggest that a possible reason to explain this finding is that when the PTX:DXR mixture is administered in the free form at a 1:10 molar ratio, despite the differences in the pharmacokinetics of the two drugs, the combination reaching the tumor site still contains DXR in higher proportions compared to PTX. As no significant cytotoxicity difference was observed in *in vitro* studies for 1:1 and 1:10 PTX:DXR molar ratio combinations against the 4T1 cell line, we suggest that some ratio of PTX:DXR within this range may have reached the tumor region, leading to similar antitumor efficacy, as observed herein. However, further biodistribution studies are necessary to confirm this hypothesis. It is known that the murine mammary carcinoma 4T1 causes a profound leukemoid reaction with splenomegaly in mice [38]. The leucocyte quantification (Table 2) and spleen size evaluation (Fig. 6) in the present study corroborate the data on tumor volume and IR. Animals in the control group presented high concentrations of total leucocyte (61.2 ± 8.3 × 10^9/L) and treatments with free PTX at dose of 0.85 m/Kg or 8.54 mg/kg were not able to suppress this leukemoid reaction ($P > 0.05$), as the total leucocyte amount quantified was equal to 69.5 ± 9.6 x10^9/L and 64.1 ± 23.9 × 10^9/L, respectively ($P < 0.05$). Treatments containing DXR significantly lowered the amount of total leucocyte compared to the control group. These results are in agreement with those obtained for tumor growth suppression. Animals treated with free DXR (5.45 mg/kg) presented a total leucocyte amount of 5.7 ± 1.9 x10^9/L, while those treated with free PTX:DXR or LCFL-PTX/DXR (PTX 0.85 mg/kg + DXR 5.45 mg/kg) presented a total leucocyte amount of 4.1 ± 0.6 × 10^9/L and 5.3 ± 1.4 × 10^9/L, respectively. Another interesting finding relates to the neutrophil-to-lymphocyte ratio (NLR) for the animals in groups receiving the different treatments containing DXR. It is known that elevated NLR value is strongly associated with poor survival of breast cancer patients and can be regarded as a predictive and prognostic factor for these patients [39,40]. Animals treated with the free mixture of PTX:DXR presented a statistically higher NLR value (3.5 ± 0.9) compared to the animals treated with free DXR (1.5 ± 0.6) or LCFL-PTX/DXR (1.5 ± 0.3; $P < 0.05$). Regarding the spleen size of animals in the different groups, splenomegaly was observed for animals in the control group and treated with free PTX at a dose of 0.85 mg/kg or 8.54 mg/kg, and free DXR at a dose of 5.45 mg/kg. This reaction was not observed in animals treated with free PTX:DXR or LCFL-PTX/DXR (PTX 0.85 mg/kg + DXR 5.45 mg/kg).

Table 1
Tumor growth inhibition ratio (IR) after administration of different treatments by IV route to Balb/c female mice transplanted subcutaneously with 4T1 breast cancer cells. The number of animals was equal to seven in groups treated with NaCl 0.9% (w/v) or LCFL-PTX/DXR, and six in the other groups.

Treatment	Dose(mg/kg)	IR(%)
NaCl 0.9% (w/v)	–	–
Free PTX	0.85 mg/kg	17.5
Free PTX	8.54 mg/kg	18.4
Free DXR	5.45 mg/kg	37.6
Free PTX:DXR	PTX 0.85 mg/kg + DXR 5.45 mg/kg	66.9
LCFL-PTX/DXR	PTX 0.85 mg/kg + DXR 5.45 mg/kg	66.5

3.5.1. Tumor histology and metastasis evaluation

The tumor cells presented a solid arrangement, round to ovoid nucleus, and abundant eosinophilic cytoplasm. Accentuated nuclear pleomorphism was observed with the presence of multiple and prominent nucleoli. Tumors presented ulceration and necrosis, irrespective of the treatments as can be observed in Fig. 7. The main differences were related to the size of the tumors as well as the extension of the necrotic areas, and the proportion of viable cells. The smallest tumors were those obtained from animals treated with either free PTX:DXR or PTX:DXR co-encapsulated in liposome. Intratumoral necrotic areas were larger and a lower proportion of viable cells was observed in tumors from animals treated with free DXR (5.45 mg/kg) or LCFL-PTX/DXR (PTX 0.85 mg/kg + DXR 5.45 mg/kg) compared to the control group and animals treated with free PTX at a dose of 0.85 mg/kg or 8.54 mg/kg, or even with the mixture of free PTX/DXR (PTX 0.85 mg/kg + DXR 5.45 mg/kg).

The 4T1 mammary carcinoma is known to be highly tumorigenic, invasive, and able to spontaneously metastasize from the primary tumor to multiple distant sites, closely resembling metastatic breast cancer in human patients [42,43]. Therefore, we evaluated the lungs, liver, heart, kidneys, and spleen of animals in the different groups for metastatic foci. It is known that the main metastatic targets of 4T1 tumor are the lungs and liver [44], and in the present work, animals in all groups presented metastatic foci in the lungs. The main difference was regarding the number of pulmonary metastases, which was higher

Table 2
White blood cell count, neutrophil and lymphocyte percentages and neutrophil to lymphocyte ratio of Balb/c female mice bearing 4T1 breast tumor after different treatments*.

Parameters		Treatments					
	Reference values (range) [41]	NaCl 0.9% (w/v) solution	Free PTX (0.85 mg/kg)	Free PTX (8.54 mg/kg)	Free DXR (5.43 mg/kg)	Free PTX:DXR (PTX 0.85 mg/kg + DXR 5.43 mg/kg)	LCFL-PTX/DXR (PTX 0.85 mg/kg + DXR 5.43 mg/kg)
Total leucocyte (10^9/L)	1.4–4.8	61.2 ± 8.3	69.5 ± 9.6	64.1 ± 23.9	5.7 ± 1.9[a]	4.1 ± 0.6[a]	5.3 ± 1.43[a]
Neutrophils (%)	11–29	71.7 ± 2.1	72.2 ± 3.5	81.0 ± 1.8 [a]	57.0 ± 11.2[b]	76.0 ± 3.6	57.3 ± 5.7[a,b]
Lymphocytes (%)	65–87	23.3 ± 3.2	25.8 ± 4.4	15.5 ± 2.7[a]	42.3 ± 11.8[a,b]	23.0 ± 5.0	39.7 ± 4.7[a,b]
NLR	–	3.1 ± 0.5	2.9 ± 0.6	5.4 ± 0.9[a]	1.5 ± 0.6[a,b]	3.5 ± 0.9	1.5 ± 0.3[a,b]

* The number of animals was equal to seven in groups treated with NaCl 0.9% (w/v) or LCFL-PTX/DXR, and six in the other groups. NLR signifies neutrophils to lymphocites ratio.
[a] = differs statistically from control group.
[b] = DXR or LCFL-PTX/DXR treatments differ statistically from free PTX:DXR treatment; ANOVA, $p < 0.05$.

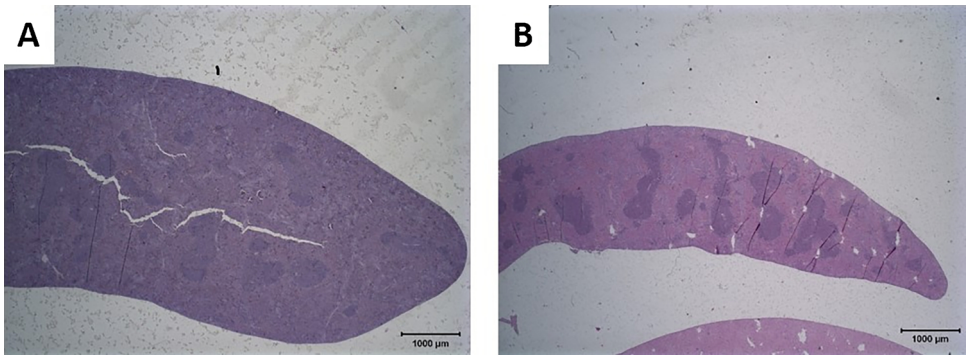

Fig. 6. Photomicrographs of spleen of animal in the (A) control group showing evident splenomegaly or (B) treated with LCFL- PTX/DXR (0.85 mg/kg + DXR 5.45 mg/kg) with normal size. Amplification 2×.

for the control group (8.6 ± 4.3). A tendency to reduce the number of pulmonary metastases was observed for animals treated with free PTX at a dose of 0.85 mg/kg (3.0 ± 2.2) or 8.54 mg/kg (4.2 ± 3.1), although this was not significantly different from the control group ($P > 0.05$). However, animals treated with free DXR (1.2 ± 0.5), the mixture of free PTX:DXR (1.4 ± 0.5), or LCFL-PTX/DXR showed a significant reduction in the number of metastases to the lungs (2.2 ± 1.2) ($P < 0.05$). Metastatic foci in the liver were observed for animals in the control group, and those treated with the different doses of free PTX or with free DXR. In the case of animals treated with free PTX either at 0.85 mg/kg or 8.54 mg/kg, multiple metastatic foci were observed. For animals treated with free DXR, rare metastatic foci were observed in only 2/6 animals, indicating a better ability of this treatment to control metastasis progression. Furthermore, the addition of PTX to the DXR treatment further improved the metastasis control. Treatments with the mixture of free PTX:DXR or LCFL-PTX/DXR

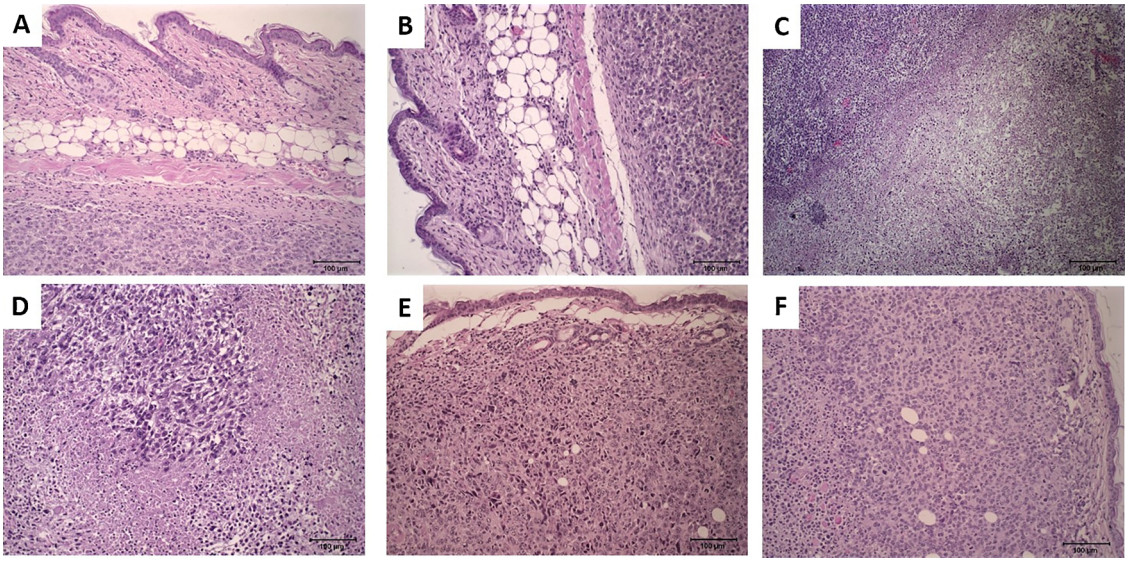

Fig. 7. Photomicrographs of tumor tissue of animal in the (A) control group or (B) treated with free PTX (0.85 mg/kg), (C) free PTX (8.54 mg/kg), (D) free DXR (5.43 mg/kg), (E) free PTX + DXR (0.85 mg/kg + DXR 5.45 mg/kg) or (F) LCFL-PTX/DXR (0.85 mg/kg + DXR 5.45 mg/kg). Amplification 20×.

Table 3
Metastatic foci in lungs, liver, and heart after intravenous administration of the different treatments to Balb/c female mice transplanted subcutaneously with 4T1 breast cancer cells. Data shown represent the mean ± SD.

	Lungs			Liver		Heart	
	Animals with metastasis	Number of pulmonary metastasis	Extension of the metastasis	Animals with metastasis	Extension of the metastasis	Animals with metastasis	Extension of the metastasis
Control	7/7	8.6 ± 4.3	Extensive	4/7	Multiple foci	4/7	Extensive
Free PTX (0.85 mg/kg)	4/6	3.0 ± 2.2	Extensive	6/6	Multiple foci	1/6	Extensive
Free PTX (8.54 mg/kg)	5/6	4.2 ± 3.1	Extensive	6/6	Multiple foci	1/6	Extensive
Free DXR (5.45 mg/kg)	4/6	1.2 ± 0.5[a]	Small	2/6	Rare foci	0/6	–
Free PTX:DXR (PTX 0.85 mg/kg + DXR 5.45 mg/kg)	5/6	1.4 ± 0.5[a]	Small	0/6	–	0/6	–
LCFL-PTX/DXR (PTX 0.85 mg/kg + DXR 5.45 mg/kg)	7/7	2.2 ± 1.2[a]	Small	0/7	–	0/7	–

[a] = differs statistically from control group. ANOVA, $p < 0.05$.

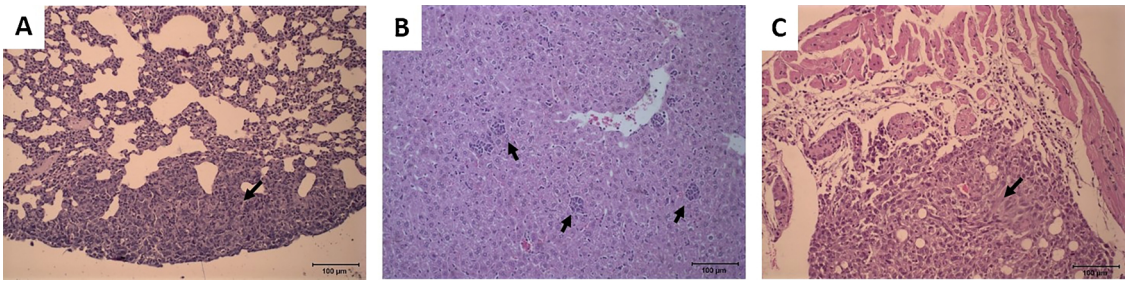

Fig. 8. Metastatic foci in lung (A), liver (B) and heart (C). Amplification 20×.

completely suppressed the metastization to the liver, since no focus was observed in the liver of animals of these groups. Cardiac metastatic foci were observed in 4/7 animals in the control group and 1/6 animals treated with free PTX (0.85 mg/kg or 8.54 mg/kg), while treatments with free DXR and the mixture of free PTX:DXR or LCFL-PTX/DXR completely suppressed the metastization to the heart. No metastatic focus was observed on the kidneys and spleen of animals of any group of treatment. Table 3 presents the number of animals that had metastatic foci in the lungs, liver, and heart after different treatments as well as the extension of the metastatic foci, while Fig. 8 illustrates metastatic foci in each of these organs.

3.6. Determination of the effect of the different treatments on plasma vascular endothelial growth factor levels

Metronomic chemotherapy is defined as the administration of chemotherapeutic agents in small doses on a frequent schedule (daily, several times a week, or weekly). This treatment strategy has also been called 'antiangiogenic chemotherapy', as it was initially reported to act through antiangiogenic mechanisms [45,46]. One of these mechanisms consists of decreasing VEGF plasma concentrations [47]. The down-regulation of VEGF expression is one of the mechanisms that contribute to the antiangiogenic activity of PTX [48]. Treatment with free PTX at a dose of 0.85 mg/kg was the only one to reduce significantly the VEGF level (37.8 ± 2.6 pg/mL) when compared to the control group (53.6 ± 6.5 pg/mL; $P < 0.05$). It is known that the mechanism of action of an anticancer agent can significantly differ depending on the administration dose and schedule [46]. When the free PTX dose was enhanced to 8.54 mg/kg, no reduction of the VEGF levels (50.4 ± 6.1 pg/mL) was observed ($P > 0.05$). Treatments with free DXR at a dose of 5.45 mg/kg (50.0 ± 8.4 pg/mL); free PTX:DXR at a dose of 0.85 mg/kg and 5.45 mg/kg, respectively, (57.9 ± 8.7 pg/mL); or LCFL-PTX/DXR at the same dose (55.5 ± 6.3 pg/mL) also did not reduce VEGF levels compared to the control group ($P > 0.05$).

3.7. Toxicity evaluation

Body weight loss can be used to measure drug-induced toxicity. Animals of the control group as well as animals receiving free PTX treatment either at a dose of 0.85 mg/kg or 8.54 mg/kg gained weight during the whole experiment, with no difference between these groups ($P > 0.05$), as shown in Fig. 9. The different treatments containing DXR presented higher toxicity to the mice. Significant weight loss ($P < 0.05$) was observed for mice receiving free DXR (5.45 mg/kg); free PTX:DXR or LCFL-PTX/DXR (PTX 0.85 mg/kg + DXR 5.45 mg/kg), starting from D6 until the end of experiment. The treatment with the mixture of free PTX:DXR (PTX 0.85 mg/kg + DXR 5.45 mg/kg) led to significantly higher weight loss compared to the treatment with free DXR alone on D9 and D12. Additionally, this treatment was the only one that led to a weight loss superior to 20% on D12, considered an indication for euthanasia to fulfill the humane endpoints in animal research [49]. This indicates that the addition of PTX to the DXR treatment enhances its toxicity. It is interesting to note that for the treatment of animals with LCFL-PTX/DXR (PTX 0.85 mg/kg + DXR 5.45 mg/kg), the weight loss did not differ from that observed for free DXR treatment on any of the experimental days ($P > 0.05$). It was also significantly lower at the end of the experiment compared to that observed for the treatment with the mixture of free PTX:DXR ($P < 0.05$). These findings suggest that the co-encapsulation of PTX and DXR in liposomes allows for a reduction of the toxicity of the combination.

Concerning hematological parameters, a better tumor inhibition for animals treated with free DXR, mixture of free PTX:DXR, and LCFL-PTX:DXR based on the total leukocyte quantification was observed, as previously explained in Section 3.5. Other hematological findings consisted of a significant enhancement of neutrophils and reduction of lymphocytes resulting in higher NLR for animals that received treatment with free PTX at a dose of 8.54 mg/kg compared to the control group. These animals also presented lower concentrations of red blood cells and hemoglobin compared to the control group ($P < 0.05$).

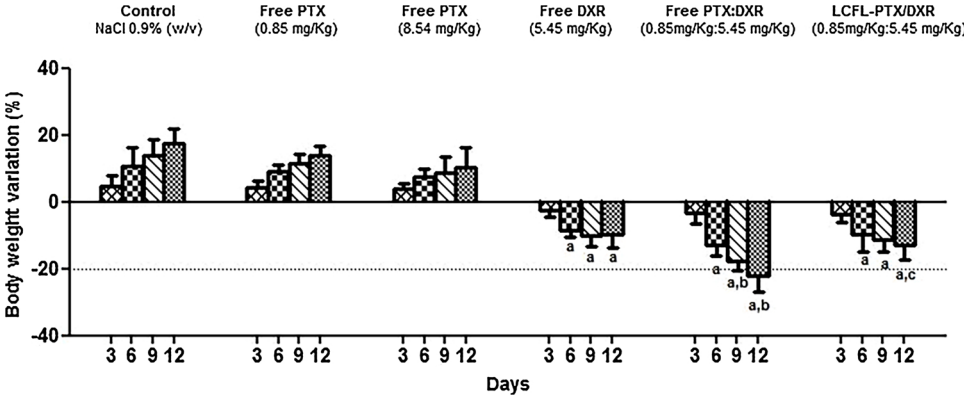

Fig. 9. Body weight variation of Balb/c female mice transplanted subcutaneously with 4T1 breast cancer cells observed during 12 experimental days. Intravenous administration of NaCl 0.9% (w/v), free PTX (0.85 mg/kg or 8.54 mg/kg), free DXR (5.45 mg/kg), free mixture of PTX:DXR or LCFL-PTX/DXR at 1:10 molar ratio (PTX 0.85 mg/kg + DXR 5.45 mg/kg) occurred on days 0, 3, 6 and 9. Data shown represent the mean ± SD of three independent experiments. The number of animals was equal to seven in groups treated with NaCl 0.9% (w/v) or LCFL-PTX/DXR, and six in the other groups. [a] = differs statistically from control group; [b] = differs statistically from free DXR treatment; [c] = differs statistically from free PTX:DXR treatment. ANOVA, $p < 0.05$.

Table 4
Hematological parameters of Balb/c female mice bearing 4T1 breast tumor after different treatments*.

Parameters		Treatments					
	Reference values (range) [41]	NaCl 0.9% (w/v) solution	Free PTX (0.85 mg/kg)	Free PTX (8.54 mg/kg)	Free DXR (5.43 mg/kg)	Free PTX:DXR (PTX 0.85 mg/kg + DXR 5.43 mg/kg)	LCFL-PTX/DXR (PTX 0.85 mg/kg + DXR 5.43 mg/kg)
Red blood cells (10^{12}/L)	7.1–9.5	6.4 ± 0.3	6.9 ± 0.7	5.1 ± 0.9[a]	4.9 ± 0.8[a]	5.9 ± 0.4	5.8 ± 0.4
Hemoglobin (g/L)	11.6–15.8	12.8 ± 0.8	14.1 ± 1.9	10.2 ± 2.3[a]	8.7 ± 1.9[a]	11.2 ± 1.1	10.9 ± 0.9
Hematocrit (%)	37.4–51.7	31.5 ± 1.7	34.9 ± 2.9	28.9 ± 5.3	24.8 ± 4.2[a]	29.3 ± 1.7	28.2 ± 1.8
Platelets (10^9/L)	325–888	498.6 ± 139.6	404.5 ± 97.3	570.3 ± 89.6	225.3 ± 46.8[a]	429.8 ± 135.4	428.7 ± 128.4

* The number of animals was equal to seven in groups treated with NaCl 0.9% (w/v) or LCFL-PTX/DXR, and six in the other groups.
[a] = differs statistically from control group. ANOVA, $p < 0.05$.

Animals that received free DXR treatment (5.45 mg/kg) presented lower red blood cell, hemoglobin, hematocrit, and platelet counts compared to the control group ($P < 0.05$) as presented in Table 4.

The histopathological analyses of the organs revealed cardiotoxicity for the treatments with free DXR (5.45 mg/kg) and free PTX:DXR at 1:10 molar ratio (PTX 0.85 mg/kg + DXR 5.45 mg/kg). Hearts of all animals receiving those treatments presented mild hyaline multifocal degeneration. Three out of 6 animals treated with free DXR also presented cardiac steatosis. Focal tubular necrosis was observed in the kidneys of 2/6 animals treated with free PTX (8.54 mg/kg) and 1/6 animals treated with free DXR (5.45 mg/kg). Fig. 10 illustrates the toxicity signs observed in the kidneys and heart. No sign of toxicity was observed in the lungs and liver of animals of any group. The spleen of animals of the control group as well as those treated with free PTX at a dose of 0.85 mg/kg or 8.54 mg/kg and free DXR at a dose of 5.45 mg/kg presented white and red pulp hyperplasia, which was less severe in the last group.

4. Discussion

We described herein the results of the *in vitro* effects of treatments with PTX, DXR, or its combinations at different molar ratios against the 4T1 murine breast cancer cell line, as well as the findings of the *in vivo* experiments carried out to investigate the antitumor activity and toxicity of LCFL-PTX/DXR in Balb/c mice bearing 4T1 breast tumor. *In vitro* experiments consisted of the evaluation of cytotoxicity, NMA, and migration of 4T1 cells exposed to the treatments with free PTX, free DXR, or its combinations in free form at different molar ratios (PTX:DXR = 10:1, 1:1, or 1:10). The mixtures of free PTX:DXR combined at 1:1 or 1:10 molar ratios have shown to be the most cytotoxic treatments, not differing between them, while the combination at a 10:1 molar ratio was less cytotoxic than DXR treatment alone. The NMA revealed that the PTX treatment led to similar amounts of LR and LI + I nuclei, while all other treatments resulted predominantly in an increased percentage of LR nuclei. These results reveal that the addition

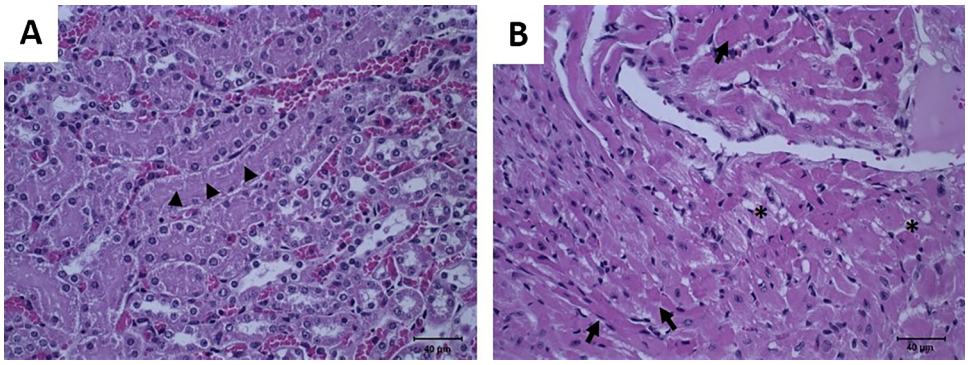

Fig. 10. Focal tubular necrosis (A, arrow heads) observed in the kidneys of animals that received treatments with free PTX (8.54 mg/kg) or free DXR (5.45 mg/kg); mild hyaline multifocal degeneration (B, arrow) observed in the hearts of animals that received treatments with free DXR (5.45 mg/kg) or free PTX:DXR (PTX 0.85 mg/kg + DXR 5.45 mg/kg) and steatosis (B, asterisk) for those that received free DXR treatment (5.45 mg/kg). Amplification 20×.

of even small amounts of DXR to PTX treatment, such as in the PTX:DXR combination at a 10:1 molar ratio (636 nM: 63 nM), prevents the effects of the PTX treatment on nuclear morphology. This dominance of the effect produced by DXR treatment over the PTX treatment has been previously reported for colon cancer cells [50].

The migration assay showed that the DXR treatment alone was not able to inhibit 4T1 cell migration. The addition of small amounts of PTX to the DXR treatment allowed a significant migration inhibition. This emphasizes the benefits of the combination, as the metastasis represents a huge problem of the cancer treatment, indicating poor prognosis and having dramatic effects on the survival of patients [36]. It is known that anticancer activity against a broad range of tumor cell lines enhances the chances of a successful clinical outcome for a determined compound or combination [12]. The *in vitro* studies herein presented for the 4T1 cell line show a similar activity for both 1:1 and 1:10 combinations of PTX:DXR. However, previous studies using A549, B16, HepG2, KB, MDA-MB-231, and ES-2 cell lines reported synergism for PTX:DXR combinations in which DXR is present in higher proportions compared to PTX [51–53]. For this reason, we considered the 1:10 PTX:DXR combination to be more predictive of clinical efficacy, choosing it as the therapeutic option to be investigated *in vivo*.

LCFL-PTX/DXR retained the cytotoxicity properties of the mixture of free drugs at the same ratio, as no statistical difference was observed for the determined IC_{50} value. Thus, we evaluated the antitumor efficacy and toxicity of this formulation (PTX 0.85 mg/kg + DXR 5.45 mg/kg) and compared it to the treatments with different doses of free PTX (0.85 mg/kg and 8.54 mg/kg); free DXR (5.45 mg/kg); and the mixture of free PTX:DXR (PTX 0.85 mg/kg + DXR 5.45 mg/kg). Similar tumor IR values were found for treatments with free PTX at low dose (IR = 17.5) and high dose (IR = 18.4). The leucocyte quantification revealed no difference between groups treated with different doses of free PTX and the control group, corroborating the low tumor IR found, as this profound leukemoid reaction is correlated with the 4T1 tumor burden. Animals receiving these treatments also presented splenomegaly, similar to the animals of the control group, which also presented the tumor burden [38]. These mice also presented extensive metastatic foci in the lungs, liver, and heart, similar to those observed for the control group. As it can be observed, enhancing the PTX dose to 8.54 mg/kg did not enhance its efficacy when compared to the administration of a low PTX dose (0.85 mg/kg). Similar findings were reported by Jiang and coworkers (2010), who demonstrated that a low-dose metronomic paclitaxel chemotherapy scheme (i.p. 1.3 mg/kg daily) was more effective in suppressing tumor growth in a 4T1 mouse model compared to the MTD therapy (i.p. 20 mg/kg weekly). In their study, this was partly explained by the fact that the metronomic regimen displayed stronger anti-angiogenic and anti-lymphangiogenic activities compared to the MTD regimen [54]. In the present study, the treatment with free PTX at a dose of 0.85 mg/kg was the only one to reduce significantly the VEGF levels when compared to the control group. The increase in the dose of free PTX to 8.54 mg/kg or combining PTX at a dose of 0.85 mg/kg to DXR at a dose of 5.45 mg/kg either in free or co-encapsulated form did not reduce the plasma VEGF levels. The tumor IR for treatment with free DXR (IR = 37.6) was about 2-fold higher than that for treatments with free PTX. Leucocyte quantification was significantly lower compared to that of the control and splenomegaly was mild, corroborating a better efficacy when compared to the treatment with free PTX. The number of pulmonary metastases was significantly reduced for this treatment group when compared to the control group. In addition, only rare foci of liver metastasis were observed and there was no metastasis in the heart after free DXR treatment. The addition of a small amount of PTX to the DXR treatment led to increased therapeutic efficacy. The tumor IR value for the treatment with free PTX:DXR was 66.9 and that for LCFL-PTX/DXR treatment was 66.5. These treatments significantly reduced the leucocyte levels compared to that of the control group and no splenomegaly was observed. The number of pulmonary metastases was significantly reduced for these groups when compared to the control group, and there were no metastases to the liver and heart. When comparing these two groups, despite similar tumor sizes, the histophatological analysis of the tumors showed a lower proportion of viable cells in the tumor mass of animals treated with LCFL-PTX/DXR. Another interesting observation was that the NLR, strongly associated with the poor survival of breast cancer patients [39,40], was significantly lower for the animals treated with LCFL-PTX/DXR compared to the free PTX:DXR mixture treatment. It could be expected that the co-encapsulation of PTX:DXR at a fixed ratio in LCFL enhanced considerably the antitumor activity of the combination by enabling its delivery at an optimal ratio to the tumor site [13]. However, the antitumor efficacy of the mixture of free PTX:DXR and LCFL-PTX/DXR was rather similar. A possible explanation for this finding is related to the fact that for the 4T1 breast cancer cell line the alteration of the PTX:DXR molar ratio from 1:1 to 1:10 did not significantly modify its cytotoxicity. Thus, upon administration of the 1:10 ratio, the efficacy would only be compromised if the PTX:DXR ratio was altered in a way that the PTX concentration is above that of DXR, which possibly did not occur. Further studies are necessary to confirm this hypothesis. It is worth highlighting that the toxicity profile of the treatments with free PTX:DXR or co-encapsulated PTX:DXR combination in liposomes was different. Concerning body weight variations as an indicator of drug-induced toxicity, treatments containing DXR presented higher toxicity to the mice, as they led to significant weight loss compared to the control group. The treatment with the mixture of free PTX:DXR was the most toxic since it was the only one that led to a weight loss superior to 20% on D12, reaching a humane endpoint in animal research [49]. This weight loss on D12 was significantly more pronounced than that observed for animals that received free DXR or LCFL-PTX/DXR. For animals treated with LCFL-PTX/DXR, the weight loss did not differ from that observed for animals treated with free DXR on any of the experimental days. The encapsulation of the combination of PTX:DXR also contributed to a cardiotoxicity reduction, as revealed by the histopathological analysis of the heart. A mild hyaline multifocal degeneration was observed in the heart of all animals that received free DXR and free PTX:DXR mixture. Three out of 6 animals treated with free DXR also presented cardiac steatosis. No signs of cardiac toxicity were observed for animals in any other groups of treatment. These findings show that the co-encapsulation of PTX and DXR in liposomes leads to a reduction in the toxicity of the combination, enabling the co-administration of PTX and DXR and suggesting that it is more effective than the administration of DXR and PTX treatments separately at different time intervals [55,56]. The co-administration of these agents is nowadays hampered due to the pharmacokinetic interference of PTX in DXR elimination, which leads to enhanced plasma concentrations of DXR and its metabolite, doxorubicinol, also known to be highly cardiotoxic [57,58]. This pharmacokinetics interference is possibly eliminated upon co-encapsulation of the agents, and makes the LCFL-PTX/DXR a promising candidate for chemotherapy.

5. Conclusion

Our results show that the long-circulating and fusogenic liposomal formulation co-encapsulating PTX:DXR at a 1:10 molar ratio has better antitumor efficacy compared to the treatments with free PTX or free DXR and similar efficacy as compared to the mixture of free PTX:DXR (1:10 molar ratio) administered at the same dose. The great advantage of the liposomal formulation is related to its improved toxicity profile. The body weight loss for animals treated with LCFL-PTX/DXR was significantly less pronounced compared to that for animals treated with free mixture of PTX:DXR. No signs of cardiac toxicity were observed for animals treated with LCFL-PTX/DXR, while the hearts of all animals treated with the free combination presented degeneration. Thus, LCFL-PTX/DXR enables the co-administration of PTX and DXR, and the treatment of cancer with this formulation might be more effective than the administration of PTX and DXR with an interval between them.

Disclosure

The authors report no conflicts of interest in this work.

Acknowledgments

The authors would like to thank Fundação de Amparo à Pesquisa do Estado de Minas Gerais – FAPEMIG (CDS - RED-00007-14- REDE MINEIRA DE PESQUISAS EM NANOBIOTECNOLOGIA) and Conselho Nacional de Desenvolvimento Científico e Tecnológico – CNPq (306197/2014-6 and 446627/2014-3) for the financial support. The authors also thank Coordenação de Aperfeiçoamento de Pessoal de Nível Superior – CAPES for supporting Marina Santiago Franco with a scholarship.

References

[1] GLOBOCAN: Estimated Cancer Incidence, Mortality, and Prevalence Worldwide in 2012, (2014).
[2] S.A. Narod, J. Iqbal, A.B. Miller, Why have breast cancer mortality rates declined? J. Cancer Policy 5 (2015) 8–17.
[3] J. Bines, H. Earl, A.C. Buzaid, E.D. Saad, Anthracyclines and taxanes in the neo/adjuvant treatment of breast cancer: does the sequence matter? Ann. Oncol. 25 (2014) 1079–1085.
[4] Q.-W. Tan, T. Luo, H. Zheng, T.-L. Tian, P. He, J. Chen, H.-L. Zeng, Q. Lv, Weekly taxane-anthracycline combination regimen versus tri-weekly anthracycline-based regimen for the treatment of locally advanced breast cancer: a randomized controlled trial, Chin. J. Cancer 36 (2017) 27.
[5] B.I. Bodai, P. Tuso, Breast cancer survivorship: a comprehensive review of long-term medical issues and lifestyle recommendations, Perm. J. 19 (2015) 48–79.
[6] J.J. Tao, K. Visvanathan, A.C. Wolff, Long term side effects of adjuvant chemotherapy in patients with early breast cancer, Breast 24 (2015) S149–S153.
[7] J. Shi, P.W. Kantoff, R. Wooster, O.C. Farokhzad, Cancer nanomedicine: progress, challenges and opportunities, Nat. Rev. Cancer 17 (2017) 20–37.
[8] S. Shen, M. Liu, T. Li, S. Lin, R. Mo, Recent progress in nanomedicine-based combination cancer therapy using a site-specific co-delivery strategy, Biomater. Sci. 5 (2017) 1367–1381.
[9] T. Jiang, W. Sun, Q. Zhu, N.A. Burns, S.A. Khan, R. Mo, Z. Gu, Furin-mediated sequential delivery of anticancer cytokine and small-molecule drug shuttled by graphene, Adv. Mater. 27 (2015) 1021–1028.
[10] T. Jiang, R. Mo, A. Bellotti, J. Zhou, Z. Gu, Gel-liposome-mediated co-delivery of anticancer membrane-associated proteins and small-molecule drugs for enhanced therapeutic efficacy, Adv. Funct. Mater. 24 (2014) 2295–2304.
[11] D. Wu, M. Si, H.-Y. Xue, H.-L. Wong, Nanomedicine applications in the treatment of breast cancer: current state of the art, Int. J. Nanomedicine 12 (2017) 5879–5892.
[12] M.S. Franco, M.C. Oliveira, Ratiometric drug delivery using non-liposomal nanocarriers as an approach to increase efficacy and safety of combination chemotherapy, Biomed. Pharmacother. 96 (2017) 584–595.
[13] M.S. Franco, M.C. Oliveira, Liposomes co-encapsulating anticancer drugs in synergistic ratios as an approach to promote increased efficacy and greater safety, Anticancer Agents Med. Chem. (2018), https://doi.org/10.2174/1871520618666180420170124.
[14] L.D. Mayer, A.S. Janoff, Optimizing combination chemotherapy by controlling drug ratios, Mol. Interv. 7 (2007) 216–223.
[15] L.D. Mayer, Ratiometric dosing of anticancer drug combinations: controlling drug ratios after systemic administration regulates therapeutic activity in tumor-bearing mice, Mol. Cancer Ther. 5 (2006) 1854–1863.
[16] D. Zucker, Y. Barenholz, Optimization of vincristine-topotecan combination–paving the way for improved chemotherapy regimens by nanoliposomes, J. Control. Release 146 (2010) 326–333.
[17] M.-Y. Wong, G.N.C. Chiu, Liposome formulation of co-encapsulated vincristine and quercetin enhanced antitumor activity in a trastuzumab-insensitive breast tumor xenograft model, Nanomedicine 7 (2011) 834–840.
[18] T. Ciofani, T. Harasym, M.C.Y. Juan, L. Mayer, D. Cabral-Lilly, S. Xie, Abstract 5464: determination of total and encapsulated drug pharmacokinetics for CPX-351, a nanoscale liposomal fixed molar ratio of cytarabine-daunorubicin (Cyt:daun), Cancer Res. 71 (2011) 5464–5464.
[19] I.M. Shaikh, K.-B. Tan, A. Chaudhury, Y. Liu, B.-J. Tan, B.M.J. Tan, G.N.C. Chiu, Liposome co-encapsulation of synergistic combination of irinotecan and doxorubicin for the treatment of intraperitoneally grown ovarian tumor xenograft, J. Control Release 172 (2013) 852–861.
[20] Y. Liu, J. Fang, Y.-J. Kim, M.K. Wong, P. Wang, Codelivery of doxorubicin and paclitaxel by cross-linked multilamellar liposome enables synergistic antitumor activity, Mol. Pharm. 11 (2014) 1651–1661.
[21] Website, (n.d.). https://www.fda.gov/NewsEvents/Newsroom/PressAnnouncements/ucm569883.htm. (Accessed 4 June 2018).
[22] Website, (n.d.). https://www.accessdata.fda.gov/drugsatfda_docs/label/2017/209401s000lbl.pdf. (Accessed 4 June 2018).
[23] M.C. Roque, Avaliação da atividade antitumoral de lipossomas fusogênicos de circulação prolongada co-encapsulandopaclitaxel e doxorrubicina para o tratamento do câncer de mama. Master Thesis, Universidade Federal de Minas Gerais, 2017.
[24] M.R. Rasch, Y. Yu, C. Bosoy, B.W. Goodfellow, B.A. Korgel, Chloroform-enhanced incorporation of hydrophobic gold nanocrystals into dioleoylphosphatidylcholine (DOPC) vesicle membranes, Langmuir 28 (2012) 12971–12981.
[25] C.L. Roland, S.P. Dineen, K.D. Lynn, L.A. Sullivan, M.T. Dellinger, L. Sadegh, J.P. Sullivan, D.S. Shames, R.A. Brekken, Inhibition of vascular endothelial growth factor reduces angiogenesis and modulates immune cell infiltration of orthotopic breast cancer xenografts, Mol. Cancer Ther. 8 (2009) 1761–1771.
[26] Sby M. Panalytical, Liposomes and The Use of Zeta Potential Measurements to Study Sterically Stabilized Liposomes, AZoNano.com., 2005 (Accessed 4 June 2018), https://www.azonano.com/article.aspx?ArticleID=1214.
[27] J.E. Liebmann, J.A. Cook, C. Lipschultz, D. Teague, J. Fisher, J.B. Mitchell, Cytotoxic studies of paclitaxel (Taxol®) in human tumour cell lines, Br. J. Cancer 68 (1993) 1104–1109.
[28] E.C. Filippi-Chiela, M.M. Oliveira, B. Jurkovski, S.M. Callegari-Jacques, V.D. da Silva, G. Lenz, Nuclear morphometric analysis (NMA): screening of senescence, apoptosis and nuclear irregularities, PLoS One 7 (2012) e42522.
[29] I.B. Roninson, E.V. Broude, B.-D. Chang, If not apoptosis, then what? Treatment-induced senescence and mitotic catastrophe in tumor cells, Drug Resist, Updat. 4 (2001) 303–313.
[30] Prasanna Nichat, Neha Mishra, Richa Bansal, Harshaminder Kaur, Mitotic catastrophe – role in programming of cell death, Int. J. Oral Craniofacial Sci. (2016) 003–005.
[31] D.L. Morse, H. Gray, C.M. Payne, R.J. Gillies, Docetaxel induces cell death through mitotic catastrophe in human breast cancer cells, Mol. Cancer Ther. 4 (2005) 1495–1504.
[32] D.A. Gewirtz, S.E. Holt, L.W. Elmore, Accelerated senescence: an emerging role in tumor cell response to chemotherapy and radiation, Biochem. Pharmacol. 76 (2008) 947–957.
[33] P.C. Wu, Q. Wang, L. Grobman, E. Chu, D.Y. Wu, Accelerated cellular senescence in solid tumor therapy, Exp. Oncol. 34 (2012) 298–305.
[34] O. Menyhárt, H. Harami-Papp, S. Sukumar, R. Schäfer, L. Magnani, O. de Barrios, B. Győrffy, Guidelines for the selection of functional assays to evaluate the hallmarks of cancer, Biochim. Biophys. Acta 1866 (2016) 300–319.
[35] J.E.N. Jonkman, J.A. Cathcart, F. Xu, M.E. Bartolini, J.E. Amon, K.M. Stevens, P. Colarusso, An introduction to the wound healing assay using live-cell microscopy, Cell Adh. Migr. 8 (2014) 440–451.
[36] N. Kramer, A. Walzl, C. Unger, M. Rosner, G. Krupitza, M. Hengstschläger, H. Dolznig, In vitro cell migration and invasion assays, Mutat. Res. 752 (2013) 10–24.
[37] C. Hayot, S. Farinelle, R. De Decker, C. Decaestecker, F. Darro, R. Kiss, M. Van Damme, In vitro pharmacological characterizations of the anti-angiogenic and anti-tumor cell migration properties mediated by microtubule-affecting drugs, with special emphasis on the organization of the actin cytoskeleton, Int. J. Oncol. 21 (2002) 417–425.
[38] S.A. DuPre', K.W. Hunter Jr, Murine mammary carcinoma 4T1 induces a leukemoid reaction with splenomegaly: association with tumor-derived growth factors, Exp. Mol. Pathol. 82 (2007) 12–24.
[39] J. Chen, Q. Deng, Y. Pan, B. He, H. Ying, H. Sun, X. Liu, S. Wang, Prognostic value of neutrophil-to-lymphocyte ratio in breast cancer, FEBS Open Bio 5 (2015) 502–507.
[40] S.S. Faria, P.C. Fernandes Jr, M.J.B. Silva, V.C. Lima, W. Fontes, R. Freitas-Junior, A.K. Eterovic, P. Forget, The neutrophil-to-lymphocyte ratio: a narrative review, Ecancermedicalscience 10 (2016) 702.
[41] E.W. Santos, D.C. de Oliveira, A. Hastreiter, G.B. da Silva, Jackeline Beltran, M. Tsujita, A.R. Crisma, S.M.P. Neves, R.A. Fock, P. Borelli, Hematological and biochemical reference values for C57BL/6, Swiss Webster and BALB/c mice, Braz. J. Vet. Res. Anim. Sci. 53 (2016) 138.
[42] B.A. Pulaski, S. Ostrand-Rosenberg, Mouse 4T1 breast tumor model, Curr. Protoc. Immunol. (2001) Chapter 20 Unit 20.2.
[43] Z.-G. Gao, L. Tian, J. Hu, I.-S. Park, Y.H. Bae, Prevention of metastasis in a 4T1 murine breast cancer model by doxorubicin carried by folate conjugated pH sensitive polymeric micelles, J. Control. Release 152 (2011) 84–89.
[44] S.A. DuPre´, D. Redelman, K.W. Hunter, The mouse mammary carcinoma 4T1: characterization of the cellular landscape of primary tumours and metastatic tumour foci, Int. J. Exp. Pathol. 88 (2007) 351–360.
[45] R.S. Kerbel, B.A. Kamen, The anti-angiogenic basis of metronomic chemotherapy, Nat. Rev. Cancer 4 (2004) 423–436.
[46] N. André, K. Tsai, M. Carré, E. Pasquier, Metronomic chemotherapy: direct targeting of cancer cells after all? Trends Cancer Res. 3 (2017) 319–325.
[47] S.H. Aktas, H. Akbulut, N. Akgun, F. Icli, Low dose chemotherapeutic drugs without overt cytotoxic effects decrease the secretion of VEGF by cultured human tumor cells: a tentative relationship between drug type and tumor cell type response, Cancer Biomark. 12 (2012) 135–140.
[48] G. Bocci, A. Di Paolo, R. Danesi, The pharmacological bases of the antiangiogenic activity of paclitaxel, Angiogenesis 16 (2013) 481–492.
[49] E. Liu, J. Fan, Fundamentals of Laboratory Animal Science, CRC Press, 2017.
[50] M.V. Blagosklonny, R. Robey, S. Bates, T. Fojo, Pretreatment with DNA-damaging agents permits selective killing of checkpoint-deficient cells by microtubule-active drugs, J. Clin. Invest. 105 (2000) 533–539.
[51] H. Wang, Y. Zhao, Y. Wu, Y.-L. Hu, K. Nan, G. Nie, H. Chen, Enhanced anti-tumor efficacy by co-delivery of doxorubicin and paclitaxel with amphiphilic methoxy PEG-PLGA copolymer nanoparticles, Biomaterials 32 (2011) 8281–8290.
[52] H.H.P. Duong, L.-Y.L. Yung, Synergistic co-delivery of doxorubicin and paclitaxel using multi-functional micelles for cancer treatment, Int. J. Pharm. 454 (2013) 486–495.

[53] E. Markovsky, H. Baabur-Cohen, R. Satchi-Fainaro, Anticancer polymeric nanomedicine bearing synergistic drug combination is superior to a mixture of individually-conjugated drugs, J. Control Release 187 (2014) 145–157.
[54] H. Jiang, W. Tao, M. Zhang, S. Pan, J.R. Kanwar, X. Sun, Low-dose metronomic paclitaxel chemotherapy suppresses breast tumors and metastases in mice, Cancer Invest. 28 (2010) 74–84.
[55] L. Gianni, E. Munzone, G. Capri, F. Fulfaro, E. Tarenzi, F. Villani, C. Spreafico, A. Laffranchi, A. Caraceni, C. Martini, Paclitaxel by 3-hour infusion in combination with bolus doxorubicin in women with untreated metastatic breast cancer: high antitumor efficacy and cardiac effects in a dose-finding and sequence-finding study, J. Clin. Oncol. 13 (1995) 2688–2699.
[56] V. Valero, E. Perez, V. Dieras, Doxorubicin and taxane combination regimens for metastatic breast cancer: focus on cardiac effects, Semin. Oncol. 28 (2001) 15–23.
[57] L. Gianni, L. Viganò, A. Locatelli, G. Capri, A. Giani, E. Tarenzi, G. Bonadonna, Human pharmacokinetic characterization and in vitro study of the interaction between doxorubicin and paclitaxel in patients with breast cancer, J. Clin. Oncol. 15 (1997) 1906–1915.
[58] S.H. Giordano, D.J. Booser, J.L. Murray, N.K. Ibrahim, Z.U. Rahman, V. Valero, R.L. Theriault, M.F. Rosales, E. Rivera, D. Frye, M. Ewer, N.G. Ordonez, A.U. Buzdar, G.N. Hortobagyi, A detailed evaluation of cardiac toxicity: a phase II study of doxorubicin and one- or three-hour-infusion paclitaxel in patients with metastatic breast cancer, Clin. Cancer Res. 8 (2002) 3360–3368.